Pilots' Gaze Behavior During Simulated Helicopter Air-to-Air Refueling

Sven O. Schmidt
Research Engineer

Daniel H. Greiwe
Research Engineer

Tim Jusko
Research Engineer

Institute of Flight Systems, German Aerospace Center (DLR)
Braunschweig, Germany

ABSTRACT

Refueling mid air is considered as important force multiplier for e.g. conducting search and rescue operations. Due to close proximity to the tanker, the refueling hose and drogue as well as the receiver can be strongly affected by the tanker's wake. Thus, the refueling drogue extended from the tanker by a hose is often oscillating from turbulence. Contact with the tanker has to be established by positioning the receiver's refueling probe within the tanker's drogue. During qualification training pilots are instructed to not focus on the drogue, due to its oscillations. This is done since chasing the drogue often leads to over-controlling and therefore mostly to a failed contact attempt. The presented research aims for improving today's Helicopter Air-to-Air Refueling (HAAR) as well as related training efficiency by a gain of understanding in this phenomenon. Therefore, the HAAR real-time simulation scenario at German Aerospace Center's (DLR) Air Vehicle Simulator (AVES) was extended with a multi body hose and a probe/drogue contact model to enable realistic contact initiation. During a piloted campaign, a total of six pilots with different levels of HAAR experience conducted the maneuver. This paper presents an analysis of obtained eye tracking data with regards to gaze entropy, total fixation duration on defined areas of interest and corresponding time history of control inputs. Potential links between gaze entropy and perceived workload that might be observed in the data are also discussed. Results show that the metrics can highlight differences in successful and unsuccessful attempts for contact of HAAR experienced and inexperienced pilots.

INTRODUCTION

By extending the operational deployment time of rotorcraft, HAAR represents an important strategical capability. To refuel rotorcraft in-flight the probe-and-drogue method is utilized. During this maneuver the probe, attached to the rotorcraft, has to be positioned precisely within the tanker's drogue. According to experienced pilots at least one to two misses prior to successful contact are on average quite common for a single refueling attempt. After contact is established the connection has to be maintained for about 6-8 minutes, depending on the fuel flow as well as the quantity to transfer. As seen in Figure 1, taken from the AVES scenario, all of this happens in close proximity to the tanker on both tanker's and receiver's limits of their flight envelope. Moreover, the receiver can be strongly affected by the wake of the tanker's high lift configuration, typical for this maneuver. These gusts in combination with the precision required to be shown by the rotorcraft pilots form one of the most demanding flight tasks. The maneuver is often mission critical which drives psychological pressure. Although efforts in development are rising, pilot assistance for HAAR is typically limited to standard Flight Control System (FCS). At the same time upper modes of FCS, e.g. height hold, might be too sluggish for effective assistance. To mitigate demands put on the pilots, increase maneuver efficiency and reduce the risk of accidents

Figure 1. Process of refueling mid air in the developed HAAR simulation scenario

(e.g. by decreasing contact to miss ratio per refueling attempt) or designing novel pilot assistance systems, knowing pilots' behavior conducting HAAR is crucial.

This research was part of the DLR project *Future Air-to-Air Refueling* (F(AI)²R). The objective of F(AI)²R was to explore the use of simulated probe-and-drogue Air-to-Air Refueling (AAR), for fixed-wing, rotary-wing, and unmanned aircraft. Additionally, concepts for actuated refueling drogues were considered. Further efforts on pilot assistance and automation of AAR for various types of receivers will be continued in the recently started DLR project *Future Air-to-Air Refueling Augmented, Assisted and Automated Operations* (FARAO). AAR research at DLR was initiated by DLR project LUBETA, fo-

Presented at the Vertical Flight Society's 80th Annual Forum & Technology Display, Montréal, Québec, Canada, May 7–9, 2024.

cusing solely on fixed-wing aircraft (Ref. 1).

Many crew members of the rotorcraft may be involved in managing the demands of HAAR, e.g. to observe tanker proximity and communication or to prepare and monitor the fuel system. The Pilot Monitoring (PM), for example, takes on rotorcraft monitoring tasks to free the Pilot Flying's (PF) capacities. Therefore, HAAR is considered an all-eyes-out maneuver for the PF and eye tracking a promising method to gain understanding of pilots' behavior along the maneuver. This includes determination of informative Area's of Interest (AOI) and potentially obtaining further information from their gaze. In Ref. 2 comprehending pilots' gaze behavior was underlined as important aspect to understand how different scan patterns might lead pilots to miss important information. Also, experienced pilots often quoted a higher chance of missing the drogue when too much focus is put on it while reducing longitudinal separation. This leads to the hypothesis that the pilots' scan pattern could decide over an attempt for contact being successful or not. In case the more efficient scan patterns could be transferred in early training, training efficiency might also be improved. In the context of HAAR, the assumption is made that information required by the pilots is information to judge their relative position to the tanker and drogue. To find and eventually refine optimal scan patterns that retrieve this information efficiently, gaze of pilots with HAAR experience and with low respectively no HAAR experience is analyzed and compared.

By combining the environment with gaze data, the methodology of eye tracking can help to identify the visual information gathering process (Ref. 3). According to Ref. 4, the result of an eye tracking analysis is the identification of visual attention or the visual information gathering process during a specific task. The recorded gaze points can be classified in saccades, fixations, smooth pursuits or blinks (Ref. 5). While saccades are periods with relatively large and fast movements of the eye, fixations consist of the gaze points between saccades. Fixations correspond to the visual attention of an operator and are therefore of particular relevance for the identification of the visual information gathering process. Smooth pursuits or blinks were not considered for this paper. Numerous algorithms can be used to classify gaze points in saccades and fixations, e.g. velocity-, area- or dispersion-based (Ref. 6). The combination of identified fixations and the environment is achieved through the application of AOI, whereby an AOI is to be selected in such a way that it contains a specific visual information or a specific category of visual information.

Among others Ref. 2 summarized two theories to interpret gaze behavior. First the information reduction theory from Ref. 7, according to which experienced pilots have more and longer fixations on task relevant AOI and reach those areas faster than less experienced pilots. The second is the long-term working memory theory of Ref. 8. In contradiction to the first theory, experienced pilots should need less and shorter fixations to gather information. It is thought that related information stored in long-term working memory can be rapidly accessed and utilized for faster decision making. However, both theories were found to not exclude each other by Ref. 9 hypothesizing the shorter fixations of experienced pilots are common for uneventful flight. On less familiar situations, lacking a priori information, experienced pilots still seem to have longer fixations on AOI in order to solve occurring issues.

Despite HAAR being a high-speed task for rotorcraft, visual references can be seen as very similar to hover or taking-off tasks. A closer comparison might be ship deck landing on open seas. Here, environmental references are also few, except for the ship itself. During take-off and landing on a ship's deck, Ref. 10 found more fixations Out-the-Window (OTW) than Inside-the-Cockpit (ITC) for experienced pilots in comparison to less experienced pilots. Similar results were also found during a simulated navigation task by Ref. 11.

In order to find a method for task load estimation, Ref. 12 compared Electroencephalography (EEG) data and ratings on the NASA Task Load Index (TLX) with rotorcraft pilots' gaze entropy. According to the study the concept of gaze entropy can be understood as the spacial and temporal randomness shown by visual scanning. The study found a decrease in gaze entropy with increasing task load, hypothesizing a potential link to the phenomenon of attentional tunneling, discussed in e.g. Ref. 13. Yet the use of gaze entropy as a measure to quantify task load did not fully comply to their sensitivity criterion (Ref. 12). In Ref. 14 gaze entropy is further subdivided in Static Gaze Entropy (SGE) and Gaze Transition Entropy (GTE). According to Ref. 14, both might be able to quantify scanning efficiency on their own to some degree. However, taken together they were found to potentially give information on how specific conditions affect scanning behavior.

METHODOLOGY

Eye Tracking

Various tools can be used to record eye movements, with a rough distinction being made between head-worn and stationary systems. For this study, the head-worn *Eye Tracker Pro Glasses 3* by *Tobii* was used, which consists of a wearable recording unit and the glasses itself. *Tobii* uses an improved Pupil Centre Corneal Reflection (PCCR) (Ref. 15) eye tracking technique for measuring eye movement in a stereo geometry, dark pupil tracking process. Along this process, the device carrier's eyes are illuminated by 16 infrared spotlights and video recorded by 4 infrared cameras. The eye tracking glasses with its arrangement of infrared sources and cameras is presented in Figure 2.

The scene camera of *Tobii Pro Glasses 3* covers a Field-of-View (FoV) of 63° in vertical and 95° in horizontal direction. According to general information of the manufacturer (Ref. 16), eye movements are recorded with a sampling rate of 50 Hz and an accuracy of 0.6°. In investigations conducted by Ref. 17, accuracy is found to be at least 1.2°. After recording the eye's movements, raw data is processed with the *Tobii Pro Lab Software*. First, gaze data is matched with the video of the scene camera. Secondly, every sample point is identified as saccade or fixation using a velocity threshold filter

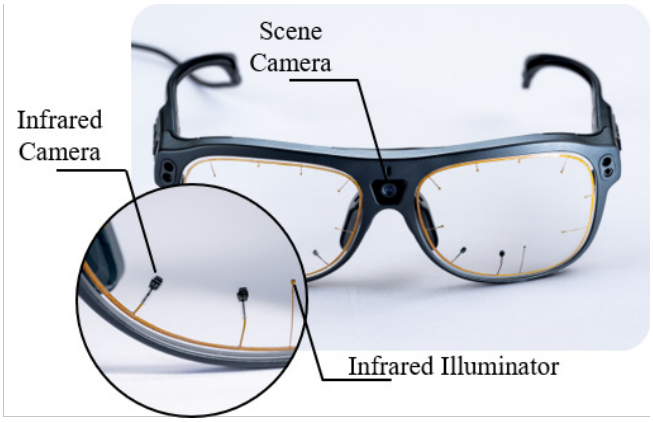

Figure 2. Tobii Pro Glasses 3

(Ref. 18), set to a threshold of 100 °/s (∼1.75 rad/s). Furthermore, the filter is set to discard all fixations with a duration shorter than 60 ms as well as to merge two fixations within a time span of 75 ms and a maximum angular change lower than 0.5°.

Gaze Entropy

So far, there are two approaches to quantify gaze dispersion. This is either *Gaze Entropy* or a *Nearest Neighbour* analysis. However, a comparison performed by Ref. 19 showed results of both measures to be very similar. The use of gaze entropy was reviewed by Ref. 14 in the further subdivided forms of Static Gaze Entropy (SGE) and Gaze Transition Entropy (GTE). While SGE considers the spacial probability distribution of fixations, GTE also includes the sequence of fixations. In this first assessment of gaze behavior during HAAR, only SGE is considered and methods of Ref. 14 are applied in the present study.

According to information theory, entropy expresses uncertainty that prevails in choice (Ref. 20). Entropy therefore describes how predictable an output as a result of choice from a set of possible options (states) is. Regarding eye movements, it is assumed that a saccade resulting in a fixation represents an independent output from the pilots' gaze regulation system (Ref. 14). Since the gaze regulation system predicts the location of a following fixation, the FoV provides the set of states that eventually can be assumed by an output. For a generated sequence of outputs from available states, entropy H is described by Equation (1) (Ref. 20). Herein p_i represents the probability for a certain state i, with n being the total number of possible states the output can assume.

$$H = -\Sigma_{i=1}^{n}(p_i)log_2(p_i) \tag{1}$$

In such contexts, the set of states describe the complexity of a system. Hence, the theoretically maximum possible complexity of a system is the entropy determined for a completely uniform distribution across all states. This indicates complete randomness or unpredictability and is implicitly described as H_{max} by Equation (2). Moreover, Equation (2) defines normalization of the observed SGE expressed by H as discussed in Ref. 14. Normalization is performed to obtain a more intuitive perception of SGE and obtained from the quotient of observed SGE H and the case of uniform distribution H_{max} expressed as a percentage. Normalized SGE ($SGE_{norm.}$) always is what is referred to throughout this investigation when values of SGE are mentioned.

$$SGE_{norm.} = \frac{H}{H_{max}} * 100\% = \frac{H}{log_2(n)} * 100\% \tag{2}$$

A scene picture represents a condensed form of the video that the eye tracking device's scene camera records from the FoV. Fixations during the time period from astern position to contact or miss were automatically mapped to the scene picture, reviewed and manually corrected if applicable. Since pilots performing HAAR have a quite rigid visual focus in the direction of the tanker without major changes, the scene picture is considered adequate to be used for SGE calculation. To quantify these states and to obtain probability distributions for SGE determination, the scene from PF's perspective is discretized. Analog to Ref. 14, fixations of the given time period are grouped into rectangular discrete bins, uniformly distributed over the visible scene. A visualization of the result is illustrated by Figure 3.

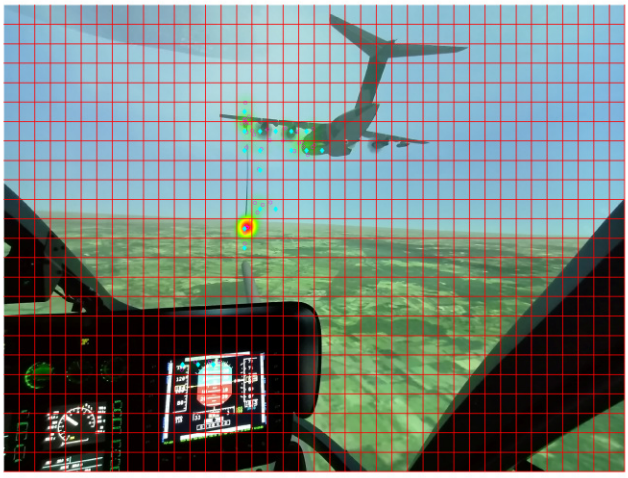

Figure 3. Scene view from pilots' perspective discretized into rectangular bins

In case of the present investigation, it was specified that bin size should not be smaller than most individual references (AOI e.g. engine, wing pod, troop door, etc.). In order to define a reasonable lower discretization limit (upper bin size) and to avoid influence of discretization artifacts, a variation in bin size was performed. Figure 4 illustrates the result in terms of normalized SGE over a scaling factor for discretization s_{Bin}. With an increase of s_{Bin} the number of bins also increases, which is resulting in smaller bins at a given size of the scene picture. The chosen 81 horizontal and 48 vertical

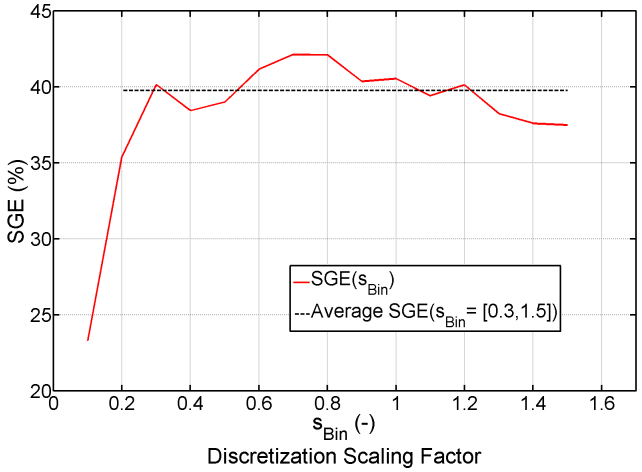

Figure 4. Effect of bin discretization on relative SGE

bins across the picture are represented by $s_{Bin} = 1$. Discretization in this form provides a reasonable bin size while resulting SGE is close to average SGE across scaling factor 0.3 to 1.5, indicated by the dashed line.

Subjective Rating Techniques

The conducted investigations with simulated HAAR require a fundamental similarity of pilot behavior compared to real flight conditions. To gain insights to the simulation fidelity of the HAAR scenario a combination of subjective rating techniques during simulation trials as well as pre and post trial pilot questionnaires had been utilized. Subjective rating techniques included the Simulation Fidelity Rating (SFR) scale, Turbulent Air Rating Scale (TS), Bedford Workload Rating (BWR) scale and are presented in the following.

SFR was first introduced in Ref. 21 and features a method for pilot self-assessment based on the transferability of training in the simulator to real flight. Ref. 21 translated the transfer of training concepts of comparative task performance and task strategy adaption to the methodology of the Cooper Harper Handling Qualities Rating Scale (Ref. 22) and refined the outcome. Simulator studies, flight tests and a workshop at the *67th Annual Forum of the American Helicopter Society* lead to the matured iteration of the 10-point ordinal scale, shown in Figure 5. Regardless of the limited number of test pilots verifying SFR in Ref. 21, further promising results of its use were presented in Ref. 23. Hence its utilization is considered appropriate for this research effort.

Ref. 24 proceeded similar to obtain the more common BWR. With an analogous decision tree methodology, the scale utilizes perceived mental spare capacity for additional tasks to quantify workload. The ratings are awarded in subsequent to flight tasks on the 10-point ordinal scale, shown in Figure 17.

In order to quantify expected and perceived turbulence in a structured way, the TS as described in Table 3 is used. The scale was initially developed for utilization in flight testing (Ref. 25) and also showed applicability in simulation trials of Ref. 26. It was selected due to its ease of application and even enabled assessments for individual phases of HAAR. Awarding TS requires the pilot to assign subjectively experienced turbulence to a linear 10-point scale. The ratings differentiate in terms of both turbulence frequency and severity.

EXPERIMENT

Simulation Facility

DLR's AVES facility is depicted in Figure 6. This simulator is equipped with four modular aircraft cabins that can be swapped out: an *Airbus A320*, a *Dassault Falcon 2000LX*, an *Eurocopter EC135*, and a single-aisle passenger cabin. A roll-on/roll-off mechanism allows these modules to be switched for utilization on either a full-scale six-degree-of-freedom hexapod motion base or a stationary base. For the presented study, the EC135 cockpit was set up on the full motion base. Both simulation platforms are equipped with a projection system comprising nine LED projectors, each offering a 1920x1200 resolution. This setup delivers a horizontal FoV of 240° and a vertical FoV ranging from −55° to 40°. Further information on the AVES simulator can be found in Ref. 27. The control configuration includes a center joystick, conventional foot pedals, and a collective that operates on a pull-for-power principle. A heads-down primary flight display and typical EC135 instruments, such as a First Limit Indicator (FLI) were provided.

Scenario Modeling

In addition to disturbances caused by the tanker wake, establishing contact is one of the most important drivers for workload during HAAR, especially when combined. Hence, the evaluation of effects of HAAR itself as well as of measures for pilot assistance requires realistic contact initiation. To provide this within the simulation, the full refueling system model described in Ref. 28 was implemented in the HAAR real time simulation environment of Ref. 29. While both studies solely utilize the refueling system model for estimation of a fixed drogue position, dynamic hose and drogue behavior is simulated in real time for the present study. The model comprises a tension controlled hose reeling mechanism, a Multi Body System (MBS) hose, a contact model enabling realistic probe/drogue interaction as well as coupling. Additionally, the refueling equipment is affected by the tanker's wake.

The Computational Fluid Dynamics (CFD) flow field representing the tanker's wake in Ref. 29 is resolved as a quasi-steady solution. Its time-invariance leads to changes in wake velocities solely as a function of Airload Computation Points's (ACP) positions relative to the tanker. As described by Refs. 29, 30 ACP are distributed over all of the rotorcraft's aerodynamically relevant components as well as the hose and drogue (e.g. rotor blade elements or lumped masses of the hose). Theoretically, this would not necessarily require great

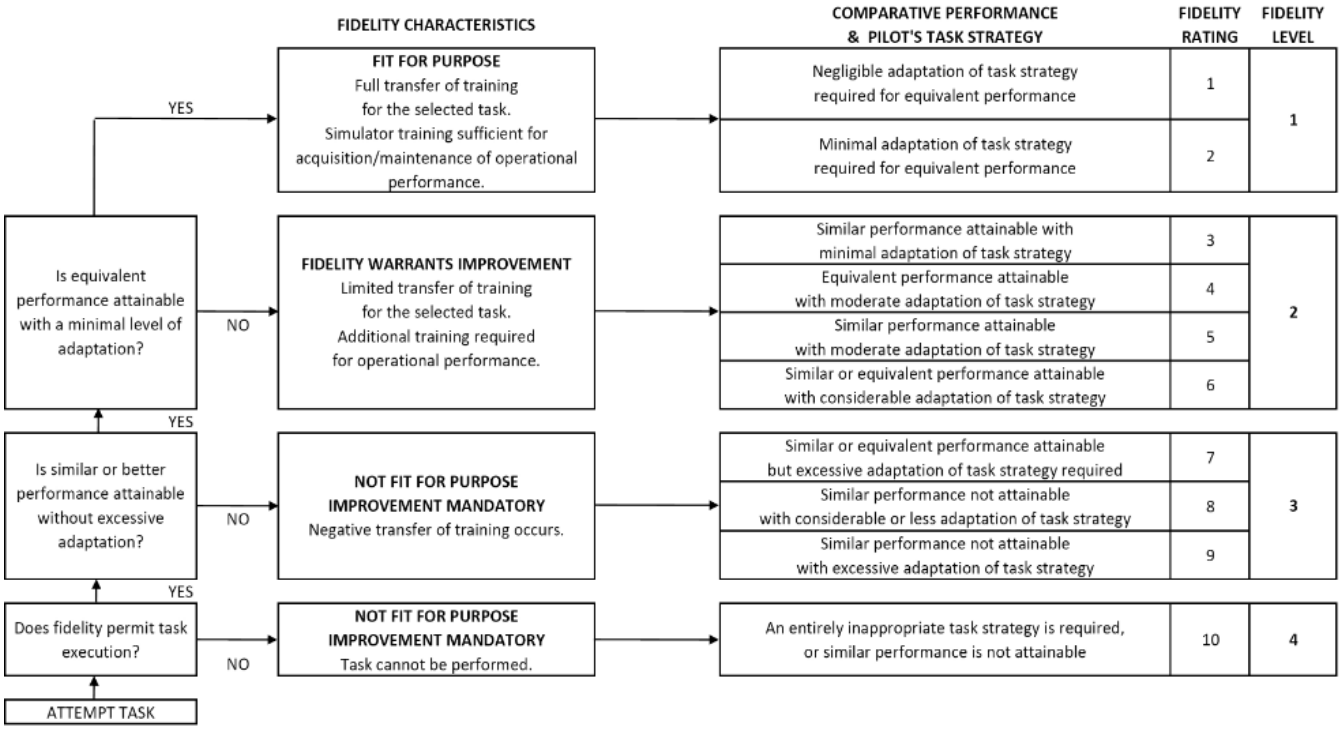

Figure 5. Simulation Fidelity Rating Scale as proposed by (Ref. 21)

Figure 6. AVES - Air Vehicle Simulator at DLR Braunschweig

pilot effort combining a trimmed helicopter with perfect adherence to the current position. Conversely, in the investigations of Ref. 29 it was assumed that unusually strong turbulence was possibly caused by the pilot's over-controlling. A recommendation of Ref. 29 to use unsteady time-dependent flow fields in the real-time simulation of HAAR or additional turbulence models with a comparable effect should therefore be considered.

Since resources for the generation of such flow fields had not been available so far, a quasi-steady tanker wake was utilized for this study as well. In contrast to Ref. 29, a flow field with a configuration of lower tanker weight (110 t) and increased flap deflection was used to achieve a smaller, visually more realistic angle of attack (6.11°). To still take unsteady effects into account, a scaled *Dryden* turbulence model was alternatively implemented for the receiver. As a stochastic turbulence model the strength of *Dryden* turbulence would be independent of location. To take differences between calm areas (e.g. refueling position) and turbulent areas (e.g. propeller downwash) automatically into account, a simple scaling of *Dryden* turbulence was additionally introduced. It is carried out by using the current absolute velocity from the tanker's wake at a reference ACP on the helicopter. This wake velocity is then multiplied with a scaling factor, that is tuned with a HAAR experienced pilot later on.

Just as the described effects on the helicopter, the drogue experiences a static deflection but shows no dynamic behavior excited by gusts. Accordingly, an additional *Dryden* model was used for the drogue's typical small amplitude higher frequency movements. In this case no spacial scaling is performed. Without the Dryden model affecting the drogue, pilots tended to rush for contact with the drogue. In the act neglecting a typical short drogue observation from *Astern Position* to estimate a quiescent phase prior to an attempt for contact.

The HAAR scenario set up in AVES represents the generic Future Military Transport Aircraft (FMTA) refueling the Generic Helicopter Model (GHM) mid air. While the aerodynamics of tanker FMTA is comparable to *Airbus' A400M* transport aircraft, its dynamics are defined by a moving point mass. Despite using the hardware of a *EC135* cockpit, the dynamics of the GHM represent a medium lift cargo heli-

copter similar to a *CH-53*. However, tanker *A400M* is not yet known to be in use for HAAR outside of the certification campaign (Refs. 31, 32). Data recordings from actual HAAR were therefore not available to be used by the authors. As a result, statements about realistic behavior of the simulation scenario can only be made on the basis of assessments by HAAR experienced pilots. Preliminary tests were carried out by pilot A to obtain initial feedback and to finetune the behavior of refueling equipment and turbulence models. The refueling equipment model was a priori configured using an HAAR parameter set derived from literature. A summary and description of these basis parameters as well as modifications to meet the properties of the utilized 120 ft hose can be found in Ref. 28. During turbulence tuning different settings of the *Dryden* scaling factor were assigned to the ranges of light turbulence (fair weather conditions, turbulence due to the tanker only) up to strong turbulence for HAAR (bad weather, general upper boundary turbulence for HAAR). For the use in subsequent evaluation campaigns a condition in between these boundaries was determined and configured.

Evaluation Procedure

A total of six pilots took part in the test campaign to evaluate the HAAR scenario in AVES. Four of the pilots from the US Army, Bundeswehr Technical Center for Aircraft and Aeronautical Equipment (WTD 61) and especially the German Air Force, had flight experience performing HAAR. The distribution over a total of five evaluation dates combined with further details of the pilots' HAAR experience, can be obtained from Table 1. In order to gather comments of the pilots' first impressions and to reduce learning effects on awarded ratings the evaluation procedure began with an extended familiarization phase. At this stage the pilots were able to freely explore the simulation with all its features. Subsequently, the simulation's fidelity was evaluated for different test cases, defined in Table 2. The four test cases reflect scenario configurations such as neglecting the spatially scaled *Dryden* model, tanker wake interference or motion cuing from the baseline configuration. The baseline configuration comprises an active motion platform as well as all the turbulence models described.

Since *Contact and Refueling Phase* is considered the most demanding phase of HAAR, the present research is focused on that phase. Hence, an evaluation run is beginning in *Observation Position* about 200 ft left and 100 ft aft the tanker's left wing tip. The dynamic hose starts reeling out at the begin of the simulation. Normally, reeling the hose out would already be performed in *Join-Up Phase*, but the receiver still has to wait for the tanker's readiness signal in *Observation Position*. Once the hose is at full trail readiness is signaled by the wing pod's light signals. It is also the pilot's signal to begin maneuvering towards *Astern Position*. Pilots with HAAR experience were asked to maneuver as they would do in real flight to gather their natural behavior, whereat pilots new to HAAR where given a introduction to standard procedures as described by Figure 7 and Ref. 29. In general, the pilots were asked to perform HAAR as they are used to it at their own discretion. No performance criteria had to be met by the pilots. Maintaining *Refueling Position* for one minute in subsequent to a successful contact forms an exception to it. The timer was started from the moment the pilot verbally signaled being stable in *Refueling Position*. After one minute expired the pilot should perform disconnect, again as usual during real flight.

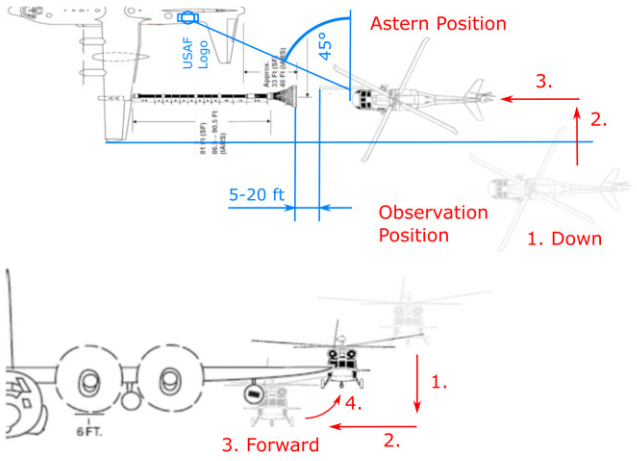

Figure 7. Maneuver sequence of the contact and refueling phase (Ref. 29)

Due to the extended familiarization phase prior to any assessment, time limitations and often several attempts necessary to achieve successful contact, one to two runs were performed for each test condition. After a completed run, the pilot was asked to award SFR, TS and BWR for each test condition. In order to obtain pilots' gaze behavior during HAAR, eye movements were recorded throughout the tests using *Tobii Pro*

Table 1. Pilot experience and participation period

Pilot	Participation Period	Overall Flight Hours	Test Pilot	HAAR experience	Last HAAR
A	May 23	3000	Yes	< 100 h	2006
B	Sep 23	2500	No	< 100 h	Mar 11
C	Oct 23	3600	No	< 10 h	Oct 13
D	Oct 23	2700	Yes	< 10 h (Simulator)	-/-
E	Oct 23	3500	Yes	0 h	-/-
F	Nov 23	2800	No	> 100 h	Feb 21

Table 2. Summary of simulation fidelity test cases

#	Test Case	Motion Cueing	Scaled Dryden	Wake Interference
1	Baseline Configuration	Enabled	Enabled	Enabled
2	No Motion	Disabled	Enabled	Enabled
3	No Scaled Dryden	Enabled	Disabled	Enabled
4	No Wake Interference	Enabled	Disabled	Disabled

Glasses 3. The device has already been utilized in Refs. 33,34 and is described in detail by Refs. 35, 36. Since pilot A performed tuning and simulation evaluation early in the investigations, no eye tracking data was recorded at that time and ratings were awarded to the unvaried baseline scenario only. Except for test case #2, characterized with a deactivated motion platform, motion cueing (Ref. 27) was provided for all of the piloted evaluations. Since the possibility of large motion excursions due to a potential passage of strong local turbulence could not be eliminated, the motion platform was set up with low-motion gains. Under real flight conditions a PM would monitor the helicopter's condition during the maneuver. The interaction between PF and PM is typically essential for the HAAR maneuver. As this could not be provided during the simulator trials, the pilots were instructed to conduct HAAR in a single-pilot configuration as natural as possible.

DISCUSSION OF RESULTS

Baseline Simulation Fidelity

As mentioned in the description of utilized rating techniques, decent simulation fidelity forms the basis for the validity of gathered objective data. The evaluation of simulation fidelity was carried out for the focused standard procedure during *Contact and Refueling Phase*, finishing with separation of probe and drogue (s. Figure 7). Figure 8 shows the SFR awarded by the pilots with prior in-flight HAAR experience (s. Table 1). For the baseline scenario with motion and all turbulence models, two ratings of SFR-2 and two ratings of SFR-4 were assigned. Both ratings are close to the margin from fidelity level 1 to 2. On average the baseline simulation scenario achieved SFR-3, which translates to a simulation fidelity level of 2. Despite the average not being a valid metric with respect to the ordinal scale, a good fidelity level 2 is regarded more realistic than a poor fidelity level 1 (s. Figure 5), considering the simulation's generic character.

The averaged awarded SFR did not exceed fidelity level 2 across all assessed variations. With additional pilot A, the baseline scenario achieved on average slightly degraded ratings. However, pilot comments quoted unrealistic calm weather conditions neglecting the turbulence models in test case #4. Since turbulence is not explicitly covered by SFR and therefore good ratings can still be awarded, the decision for the configuration to use in further investigations was made

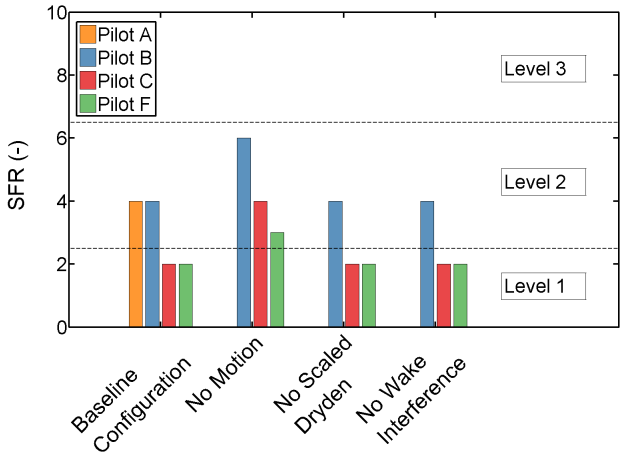

Figure 8. Simulation fidelity awarded on the Simulation Fidelity Rating Scale

up to depend on the awarded turbulence level. It is also worth to mention that the absence of motion cueing in combination with turbulence (test case #2) made a clear difference in awarded SFR.

In pre-trial pilot questionnaires the HAAR experienced pilots were asked for a range of TS ratings for actual HAAR. For each pilot awarding a distinct TS rating, the number of pilots n_{Pilots} was incremented for that rating. Since most pilots provided a range of TS, each rating given within the range was incremented. The distribution resulting from these estimations is visualized in Figure 9. According to the graph typical HAAR coincides with moderate turbulence on TS (s. Table 3). Under good weather conditions the range can also extend into the scope of light turbulence. Nonetheless, TS-6 represented the overall maximum turbulence strength for performing HAAR across all pilots.

The turbulence strength experienced in AVES was assessed by all pilots. Figure 10 shows the awarded TS ratings for each test case. On average, the baseline case resulted on the margin between moderate turbulence (TS-4) and light turbulence (TS-3). It is close to the expected turbulence range for actual HAAR, obtained from the pilots' pre-trial questionnaire (Figure 9) and symbolized by the black shaded bar. Hence, the baseline case was used for further investigation of the pilots' behavior regarding gaze movements and control inputs.

Gaze behavior during HAAR

Since contact is considered most demanding during HAAR, the following discussion is focused on the time period right before potential contact. Data from successful and unsuccessful attempts for contact will be compared. Throughout the discussion, data of inexperienced pilot E and HAAR familiar pilot F was chosen to be exemplary provided to potentially reveal major differences due to prior HAAR experience. However, data of the remaining pilots can be found in the appendix (Figures 18 to 20).

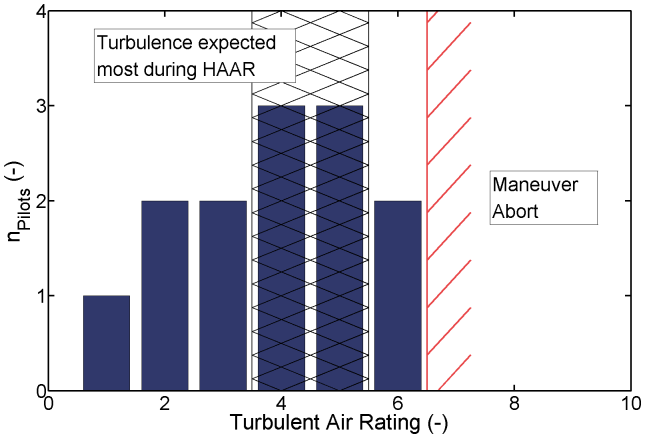

Figure 9. Turbulence ratings on the Turbulent Air Rating Scale expected for actual HAAR

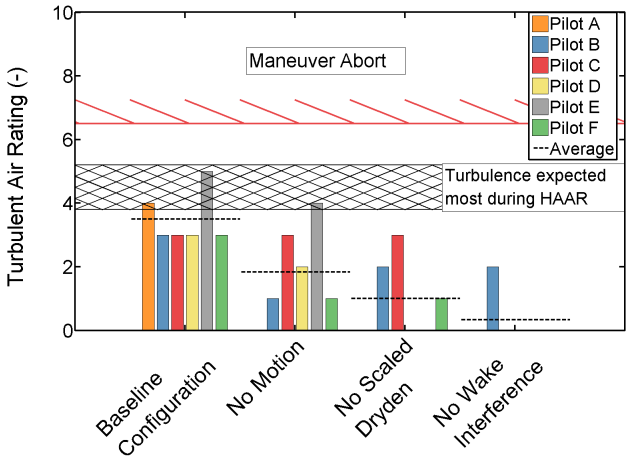

Figure 10. Turbulence ratings awarded on the Turbulent Air Rating Scale

Figure 11 shows scan patterns of pilots E and F during the period from *Astern Position* to contact or miss, defined as Time of Interest (TOI). The colored circles illustrate fixations, whereat the size of each circle indicates the fixation duration. Lines in between connect subsequent circles, symbolizing saccadic movements. The circles' numbering depicts the fixation's index within the complete scan path. Scan patterns of successful attempts for contact are colored yellow, whereat unsuccessful attempts are held in red. While pilot E's pattern seems more clustered than the one of pilot F during an unsuccessful attempt, the successful attempt shows a reversed characteristic. Other scan patterns were also observed in the remaining pilots' data (Figures 18 to 20) with comparable HAAR experience. Their gaze dispersion may qualitatively be described as in between the ones of pilot E's and F's successful attempts. As expected due to the rather strict PF/PM concept, none of the experienced pilots had fixations ITC, whereat pilot E clearly had fixations on the primary flight display.

For each pilot SGE of the representative successful and unsuccessful attempt for contact was calculated. The results are grouped per pilot and illustrated in Figure 12. For contrast reasons, data of the successful attempt is from here on colored black within diagrams, whereat the unsuccessful attempt stays red throughout the investigations. A first clearly observed characteristic is the slight to moderate drop of SGE during an unsuccessful attempt compared to a successful attempt of the same pilot. Solely pilot F drops out of this scheme. Moreover, pilot F's successful attempt also led to the lowest SGE (25.74 %) of all successful attempts. In contrast pilot E's successful attempt achieved the highest overall SGE (40.54 %), while the overall lowest SGE (20.26 %) is accompanied by pilot C's unsuccessful attempt. The drop in SGE during unsuccessful attempts might indicate some loss of information due to the lack of gaze dispersion, as hypothesized in the introduction.

In the conducted trials the HAAR experienced pilots demonstrated lower SGE than the pilots less respectively not experienced with HAAR. According to the information reduction theory (Ref. 7), more experienced pilots are expected to have more fixations of increased duration on relevant areas. This implies that fixations of experienced pilots would be more clustered over the visual scene than fixations of pilots unfamiliar with a situation. In translation to gaze entropy, it means experienced pilots are expected to have lower SGE than novices, which might be the effect observed in Figure 12.

Although not fully complying to their sensitivity criterion, Ref. 12 found a decrease in gaze entropy with an increase in task load, hypothesizing a potential link to the phenomenon of attentional tunneling (Ref. 13). A graph comparing awarded BWR with SGE, both from the HAAR simulation trials, can be seen in Figure 13. In contrast to Ref. 12 an increase of BWR with the increase in SGE can be found. Furthermore, the less experienced pilots (largest SGE) are among the highest BWR awarded. Since the task demand was not altered during the HAAR baseline trials, this might be a hint for increased gaze dispersion decreasing perceived spare capacity. However, insufficient dispersion might lead to a loss of information and could have been the case in pilot E's unsuccessful attempt. Taken together would result in a trade-off between keeping enough spare capacity for the task and gathering sufficient information form the scene. Hence, it would be beneficial for PF to cluster their gaze as much as possible, but not too much to lose information important for them.

General fixation dispersion over the FoV in form of SGE does not yet provide information on the areas pilots' are interested in during HAAR. Thus, the scene picture was divided into AOI that the pilots reported to be important in a priori interviews and pre-trial questionnaires. Additional larger areas had been introduced to collect as many fixations as possible for a complete attribution of fixation times. The definition of AOI can be obtained from the colored areas in Figure 14. Using this definition, the total fixation duration spent on each AOI can be extracted per pilot and attempt. Corresponding histograms of pilot E and F are provided in Figure 15. The bars represent total fixation duration on an AOI relative to the TOI

(a) Pilot E; Contact SGE_{yel}: 40.54 %; Miss SGE_{red}: 24.95 %

(b) Pilot F; Contact SGE_{yel}: 25.74 %; Miss SGE_{red}: 30.95 %

Figure 11. Gaze plot of pilots E and F during successful (yellow) and unsuccessful (red) attempt for contact

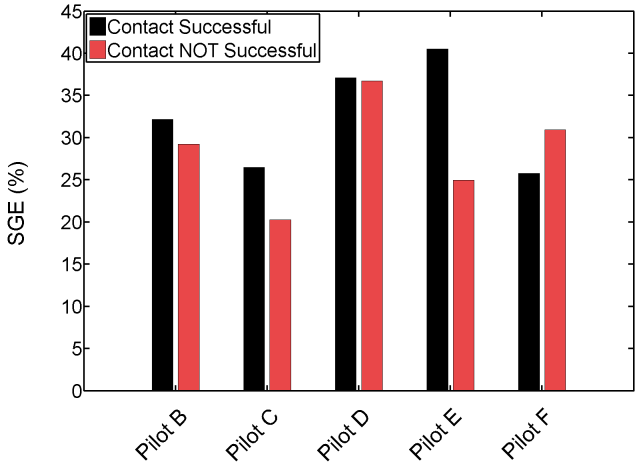

Figure 12. Resulting SGE prior to successful and unsuccessful contact of pilots

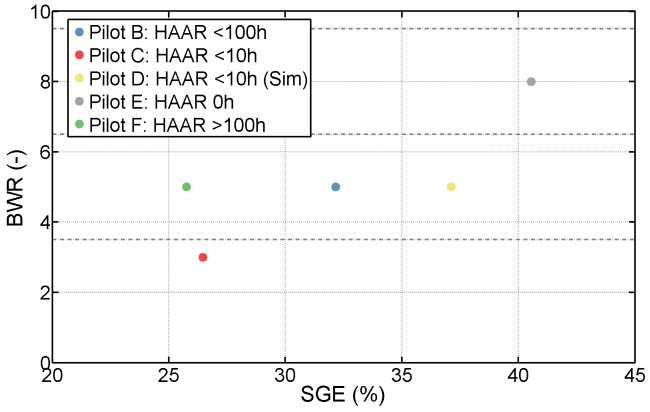

Figure 13. Observed relationship of BWR and SGE

defined by the period from astern position to contact or miss, given in percent. To find informative areas among the defined AOI, the assumption was made that experienced pilots fixate informative areas for an overall longer time period than non-informative areas. Hence, AOI were sorted from the longest to the shortest fixation duration accumulated across all experienced pilots per AOI. Examining the histograms, including the ones in Figures 18 to 20, the percentages of the total fixation duration per AOI do not add up to 100 % for each pilot. This can be attributed to the fact that saccades as well as missed data points, e.g. due to blinking, also make up some time of the TOI. However, the AOI histograms consider fixations only.

Both less experienced pilots had an overall longer fixation on the drogue during their unsuccessful attempt for contact. This draws its attention when considering that the experienced pilots spent less time fixating the drogue compared to the successful attempt. With the exception of pilot C, HAAR experienced pilots also had less overall time spend with fixations on the drogue. Pilot C accumulated 58.7 % of overall fixation duration on the drogue during the successful and 52.6 % during the unsuccessful attempt (s. Figure 19). This can be related to pilot C's scan pattern which is quite similar to the one of pilot F but with more excursions fixating the hose. Hence, only few AOI are fixated at all but therefore longer. A general drop in fixation time on AOI relevant for each particular pilot can be observed, comparing the unsuccessful with the successful attempt per pilot. Since this indicates a shift of perceived information it might be supportive to the introductory hypothesis of scan patterns that potentially decide over an attempt for contact being successful or not. In examined data, HAAR novices show tendencies to have an over proportional increase in fixation time on one AOI which therefore inevitably leads to a reduction of time fixating multiple other AOI. It spikes

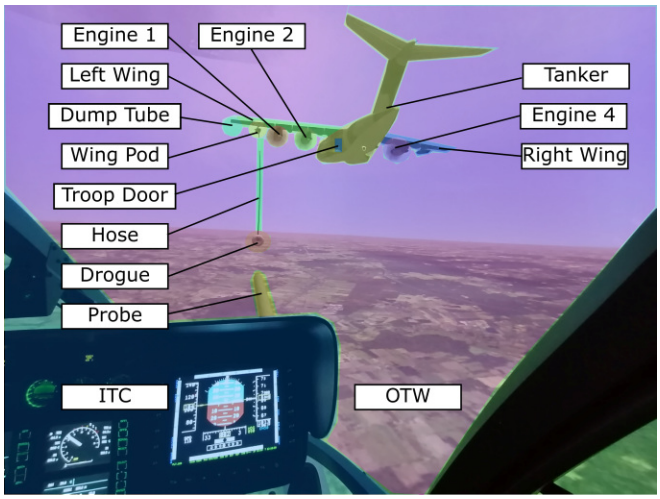

Figure 14. Definition of AOI within the HAAR scene

attention that for HAAR novices the shift of overall fixation time occurs towards the drogue. As mentioned in the introduction, this behavior is known for its adverse effects on establishing contact among HAAR experienced pilots. Consistent with expectations, none of the HAAR experienced pilots had fixations ITC since the PM would take over status monitoring during the maneuver. However, pilot E spent about 4 % of the successful attempt's TOI with fixations ITC. Examining Figure 11 these fixations can be more specifically attributed to the primary flight display.

In contrast to the doctrine of training to not focus on the drogue, it still forms the most prominent AOI across all pilots. Since the probe must be maneuvered into the drogue this seems not very remarkable. Nonetheless, it forms a contradiction between given instructions during training and actual execution of the maneuver. This leads to hypothesis that proper timing of PF's gaze is required and might be key to a successful attempt for contact. It also complies to the initial hypothesis that scan patterns might determine a successful or unsuccessful attempt for contact. For further investigations of this hypothesis Figure 16 provides time history plots of the eyes' rotational velocity along with corresponding control inputs. Again the graphs show both a successful and an unsuccessful attempt for contact per pilot. The exact moment of contact respectively miss is set to time zero ($t = 0$). Hereby, a miss is defined as the probe tip's longitudinal distance to the drogue crosses zero. The previously introduced threshold of 1.75 rad/s for the eyes' rotational velocity to be classified as saccadic movement is indicated by the horizontal blue dashed line.

In the eye velocity graphs of the Figure 16 a remarkable gap of eye's rotational velocity can be observed just shortly prior to successfully establishing contact in almost all pilots. Within this time period about 0.4 to 1.6 s prior to successful contact, they tend to fixate the drogue for 2.41 s (pilot F) to 3.27 s (pilot C). Pilot F had a fixation on the probe's tip, which was right in front of the drogue at that time. This is a shortcoming of the scene picture compared to the continuously changing scenery near the probe and drogue area observed in the scene camera's video recording. Pilots B and D are forming an exception to the mentioned gap of rotational eye velocity, where no gap to a similar extend can be found. Pilot B has a 0.95 s fixation on the drogue and subsequently a 0.43 s fixation on engine 1 just before successful contact. Pilot D, on the other hand, showed behavior more similar to pilots C, E and F. There was no continuous fixation on the drogue and only one saccade was detected shifting gaze from between the probe tip and drogue (fixation for about 1.37 s) to the drogue (fixation for about 0,46 s) with subsequent contact. Pilot E had a rather long fixation on the drogue for 6.71 s during his unsuccessful attempt, right before the miss. Since pilot E took 17.56 s from astern position to the miss, this led to the more than 60 % overall fixation duration on the drogue, observed in Figure 15.

Control behavior during HAAR

To find potential connections between gaze and control behaviors of the pilots, Figure 16 displays both time history plots of rotational eye velocity and corresponding control inputs. The data was recorded separately. Consequently, manual synchronization was performed by utilizing markers set during evaluation and the post-processing of the eye tracking data.

Once pilot E missed the drogue he commented the attempt being a miss because he was looking at the drogue and therefore made a big collective input. This input can be seen in the time history plot of pilot E's collective inputs during the unsuccessful attempt at about -2.7 s (Figure 16). Since the long fixation on the drogue mentioned before started close to -7 s, more than 4 s passed from the start of the fixation to the excessive collective input ($\Delta d_0 \approx 27\%$). From the beginning of the long fixation, an increase in amplitude over time can be observed in the collective input as well as the longitudinal cyclic input. Control amplitude not only rises over time but also over decreasing distance to the drogue. Thus, potential necessary corrections to stay aligned with the predicted drogue position at the time of contact get progressively harder to achieve. Control amplitude might be raised accordingly to correct the trajectory anyway, leading to the observed increase of control amplitude. This complies to statements pilots had given during the a priori interview describing a tendency for over-controlling due to focusing on the drogue. Moreover, it does not seem to be as pronounced during the successful attempts.

Similar observations can be made looking at time history plots of the other pilots' control inputs. It is worth to mention that pilot F already anticipated a miss in about the middle of the long fixation on the probe tip (at about -2 s). Hence, the increasing amplitude, especially in the longitudinal cyclic input, can not necessarily be attributed to the urge of final corrections in order to still achieve contact. Initiating deceleration to avoid collision with the tanker or its equipment is more likely, given the anticipation of failing contact. In subsequent to the miss, pilot F commented he had been looking on the drogue quite a lot. In contrast, large control inputs preceded pilot D's

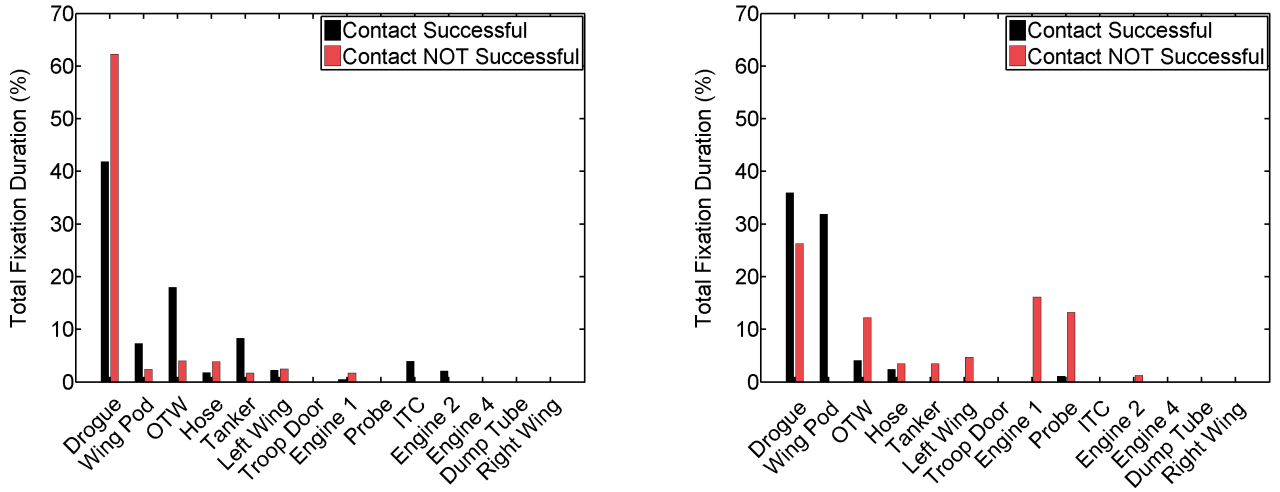

(a) Pilot E

(b) Pilot F

Figure 15. AOI histograms of pilots E and F during successful (black) and unsuccessful (red) attempt for contact

anticipation of a miss, resulting in aborting the attempt after miss.

Control frequency, on the other hand, seems to stay unchanged. Nonetheless, pilot B to D all named control frequency when asked to choose some of the main drivers for workload from a given list. In contrast pilot F did not quote frequency but control amplitude and pilot E exclusively mentioned visual references.

CONCLUSION AND OUTLOOK

The HAAR simulation scenario in AVES was extended to enable full maneuver functionalities and to achieve a more realistic experience. Therefore, a multi body hose and drogue model was implemented, including a model for probe and drogue contact. In order to attribute previous pilot comments regarding the impression of tanker wake turbulence, additional turbulence models were implemented to complement persisting tanker wake field interference. The additional models were tuned with a HAAR experienced pilot prior to any evaluation.

Utilizing subjective rating techniques, the simulation's fidelity level was assessed by further HAAR experienced pilots. The extended HAAR simulation scenario in AVES achieved a good level 2 simulation fidelity on the SFR scale (Simulation's fidelity warrants improvement but limited transfer of training for the selected task is attainable and additional training is required for operational performance). This is considered satisfactory, keeping the scenario's generic character as well as the pilots' HAAR qualification (mostly pairings of C-130 and HH-60) in mind.

After this basis was established, pilot behavior during the most challenging part of HAAR was evaluated in terms of pilot gaze and control inputs. The results of successful and unsuccessful attempts for contact between HAAR experienced and less respectively non experienced pilots were presented. Across all levels of experience, most pilots' overall fixation duration on AOI of successful attempts for contact shifted to different AOI during unsuccessful attempts. Thus, the pilots received other information, which might result in a loss of the information that is individually necessary per pilot to successfully establish contact. This supports the initial hypothesis of scan patterns that potentially decide over an attempt for contact being successful or not.

Assessment of total fixation duration from collected eye tracking data suggests that not only the duration of focus on the drogue is important for successful contact, but also the timing of when to fixate the drogue. Focusing on the drogue might lead to an increase in control amplitude especially in close proximity to it. This may not be exacerbated fast enough to the point of missing the drogue when focus is shifted to it at the latest possible time. On the other hand, focusing the drogue too late could result in loosing track of it, leading to a miss anyway.

It is recognized that the operational pilots available for the present study were only able to compare the simulation to HAAR with other tanker/receiver pairings than the generic one provided in AVES. The opportunity to compare objective data obtained from simulation with appropriate flight test data in future efforts would be beneficial for further verification of the simulation's fidelity.

Although not being easy during flight, the lack of depth perception within the simulator was again (s. Ref. 29) a major disadvantage, which could also lead to unsuccessful attempts for contact. Pilot E, for example, quoted after an unsuccessful attempt that he could just not estimate the distance to the drogue. The comment was quoted during another unsuccessful attempt that was not presented in this article.

So far, it is suggested that the proposed methods can only be used to compare the same pilot's behavior. To generalize proposed conclusions for inter-pilot comparison of behavior,

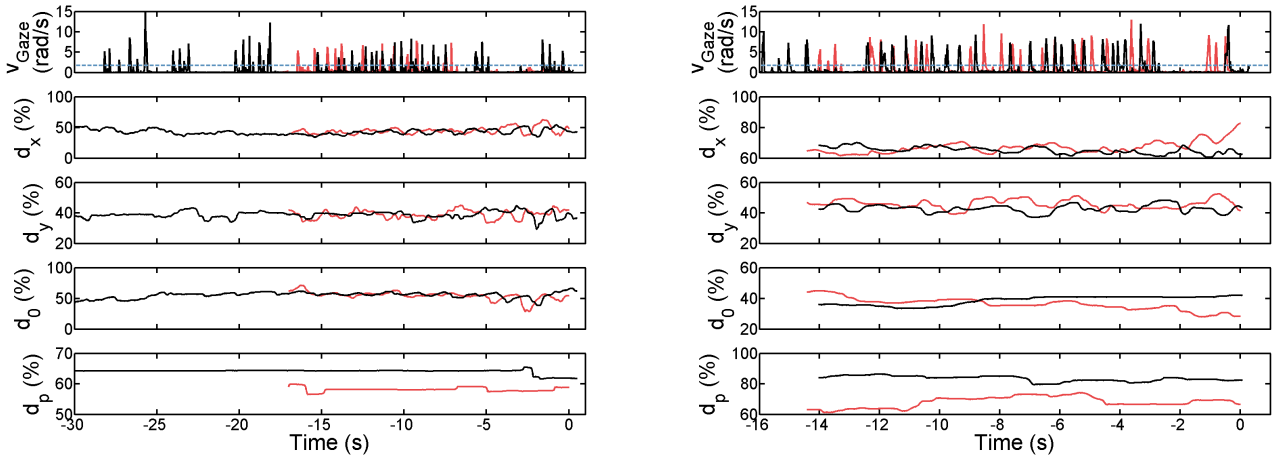

(a) Pilot E

(b) Pilot F

Figure 16. Eye's velocity and control input time history of pilots E and F during successful (black) and unsuccessful (red) attempt for contact

the data basis does not include enough pilots and specifically not enough pilots for each level of experience. Hence, further simulation trials should be carried out, to investigate the impact of fixation clustering on pilots' performance. Performance during *Contact and Refueling Phase* could be defined as the ratio of contacts per attempt.

To gain a deeper understanding on the timing of fixation sequences on relevant AOI, particularly just prior to contact, analysis of fixations per AOI and time is recommended. Additionally, the relationship between information gathering and control inputs should be further explored to find potential links and contribute to describe the phenomenon of rising control amplitude while approaching the focused drogue.

As described in the introduction, efforts on pilot assistance as well as automation for HAAR will be continued in the DLR project *Future Air-to-Air Refueling Augmented, Assisted and Automated Operations* (FARAO).

Table 3. Turbulent Air Rating Scale developed by Ref. 25

Rating	Definition	Air Condition
1	-	Flat calm
2	Light	Fairly smooth, occasional gentle displacement
3		Small movements requiring correction if in manual control
4	Moderate	Continuous small bumps
5		Continuous medium bumps
6		Medium bumps with occasional heavy ones
7	Severe	Continuous heavy bumps
8		Occasional negative "g"
9	Extreme	Rotorcraft difficult to control
10		Rotorcraft lifted bodily several hundreds of feet

ACKNOWLEDGMENTS

Funding of the presented research was provided within the scope of DLR's F(AI)²R project. The authors express their gratitude to the pilots who took part in the simulation test campaigns. Additionally, they would like to extend their thanks to those who assisted in carrying out the campaigns at the AVES test facility.

APPENDIX

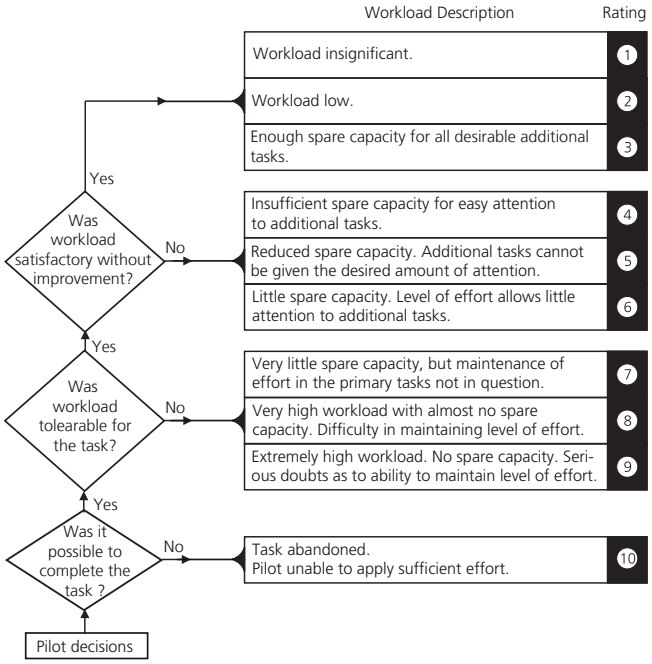

Figure 17. Bedford Workload Rating as proposed by Ref. 24

(a) Gaze Plot; SGE_{yel}: 32.16%; SGE_{red}: 29.24%

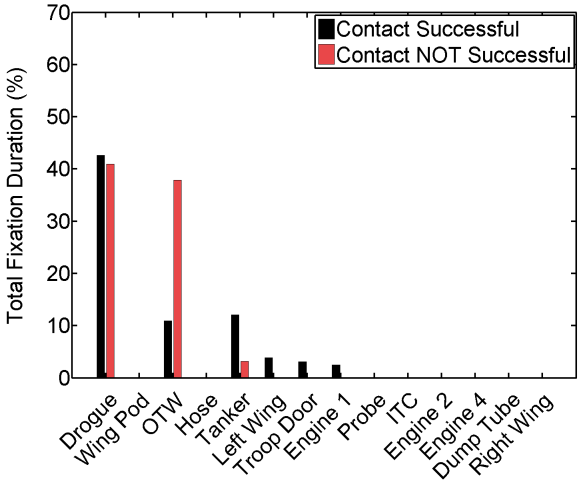

(b) AOI Histogram

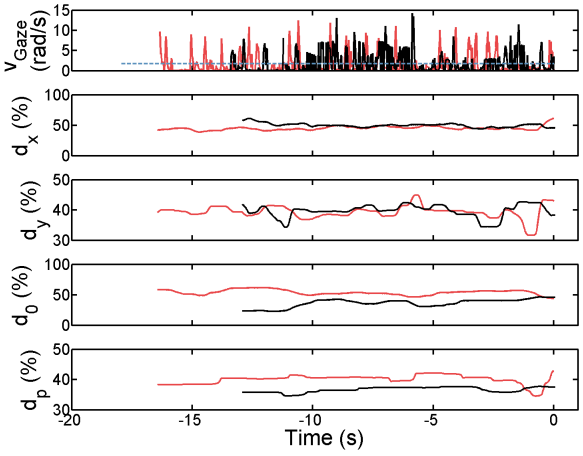

(c) Time History Diagram

Figure 18. Metrics of pilot B during successful (yellow/black) and unsuccessful (red) attempt for contact

(a) Gaze Plot; SGE_{yel}: 26.46%; SGE_{red}: 20.26%

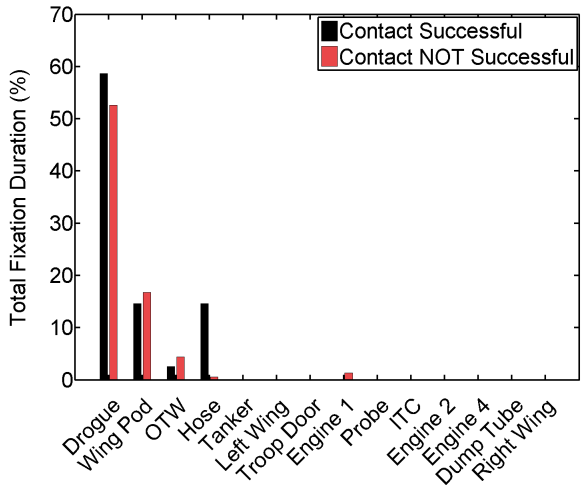

(b) AOI Histogram

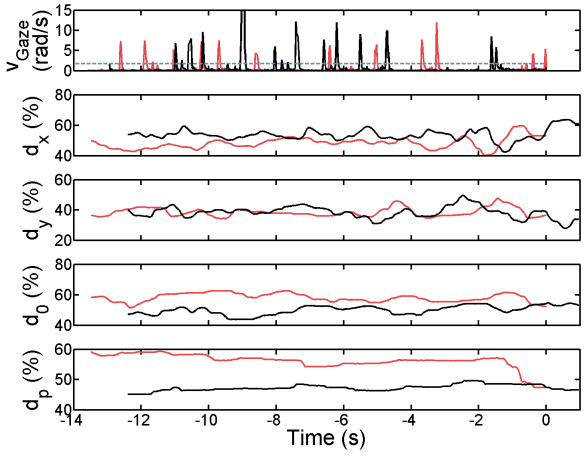

(c) Time History Diagram

Figure 19. Metrics of pilot C during successful (yellow/black) and unsuccessful (red) attempt for contact

(a) Gaze Plot; SGE_{yel}: 37.11%; SGE_{red}: 36.73%

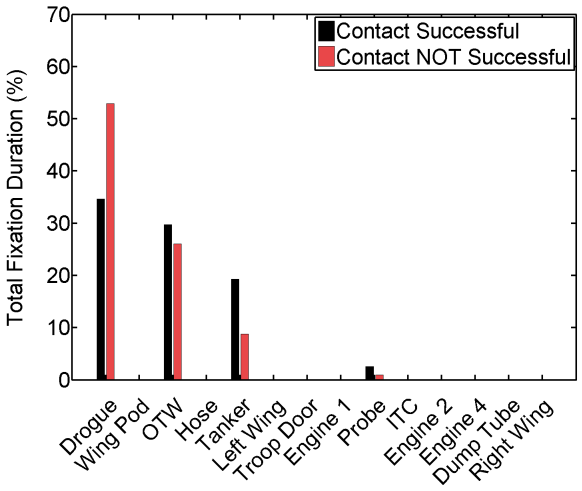

(b) AOI Histogram

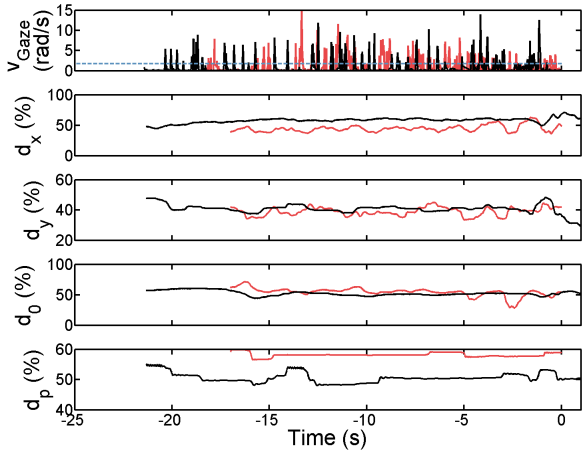

(c) Time History Diagram

Figure 20. Metrics of pilot D during successful (yellow/black) and unsuccessful (red) attempt for contact

REFERENCES

1. Fezans, N., and Jann, T., "Towards automation of aerial refuelling manoeuvres with the probe-and-drogue system: modelling and simulation," *Transportation Research Procedia*, Vol. 29, January 2018, pp. 116–134. DOI: 10.1016/j.trpro.2018.02.011.

2. Ziv, G., "The Need for Eye Tracking Studies in Helicopter Pilots: A Position Stand," Artwork Size: 6 p. Medium: application/pdf Publisher: ETH Zurich, March 2020. DOI: 10.3929/ETHZ-B-000407657.

3. Duchowski, A. T., *Eye tracking methodology: Theory and practice*, Springer London, London, 2007. DOI: 10.1007/978-1-84628-609-4.

4. Holmqvist, K., Nyström, M., Andersson, R., Dewhurst, R., Jarodzka, H., and de van Weijer, J., *Eye tracking: A comprehensive guide to methods and measures*, Oxford University Press, Oxford, New York, Auckland, 2011.

5. Reimer, B., and Sodhi, M., "Detecting eye movements in dynamic environments," *Behavior research methods*, Vol. 38, (4), 2006, pp. 667–682. DOI: 10.3758/BF03193900.

6. Salvucci, D. D., and Goldberg, J. H., "Identifying fixations and saccades in eye-tracking protocols," Paper presented at the 2000 symposium on Eye tracking research and application, Palm Beach, Florida, 6–8 November 2000, 2000. DOI: 10.1145/355017.355028.

7. Haider, H., and Frensch, P. A., "Eye Movement During Skill Acquisition: More Evidence for the Information-Reduction Hypothesis," .

8. Ericsson, K. A., and Knitsch, W., "Long-term working memory," *Psychological Review*, Vol. 102, (2), 1995, pp. 211–245. DOI: 10.1037/0033-295X.102.2.211.

9. Schriver, A. T., Morrow, D. G., Wickens, C. D., and Talleur, D. A., "Expertise Differences in Attentional Strategies Related to Pilot Decision Making," *nd ANNUAL MEETING*.

10. Robinski, M., and Stein, M., "Tracking Visual Scanning Techniques in Training Simulation for Helicopter Landing," *Journal of Eye Movement Research*, Vol. 6, (2), July 2013. DOI: 10.16910/jemr.6.2.3.

11. Kirby, C. E., Kennedy, Q., and Yang, J. H., "Helicopter Pilot Scan Techniques During Low-Altitude High-Speed Flight," *Aviation, Space, and Environmental Medicine*, Vol. 85, (7), July 2014, pp. 740–744. DOI: 10.3357/ASEM.3888.2014.

12. Diaz-Piedra, C., Rieiro, H., Cherino, A., Fuentes, L. J., Catena, A., and Di Stasi, L. L., "The effects of flight complexity on gaze entropy: An experimental study with fighter pilots," *Applied Ergonomics*, Vol. 77, May 2019, pp. 92–99. DOI: 10.1016/j.apergo.2019.01.012.

13. Christianson, S.-A., "Emotional stress and eyewitness memory: A critical review," *Psychological Bulletin*, Vol. 112, (2), 1992, pp. 284–309. DOI: 10.1037/0033-2909.112.2.284.

14. Shiferaw, B., Downey, L., and Crewther, D., "A review of gaze entropy as a measure of visual scanning efficiency," *Neuroscience & Biobehavioral Reviews*, Vol. 96, January 2019, pp. 353–366. DOI: 10.1016/j.neubiorev.2018.12.007.

15. Elvesjo, J., Skogo, M., and Elvers, G., "Method and installation for detecting and following an eye and the gaze direction thereof," U.S. Patent No. 7,572,008, 2009.

16. "Pro Lab User Manual v1.181," Vol. 1.

17. Onkhar, V., Dodou, D., and de Winter, J., "Evaluating the Tobii Pro Glasses 2 and 3 in static and dynamic conditions," *Behavior Research Methods*, 2023, pp. 1–18. DOI: 10.3758/s13428-023-02173-7.

18. Olsen, A., "The Tobii I-VT fixation filter: Algorithm Description," , 2012.

19. Maggi, P., Ricciardi, O., and Di Nocera, F., "Ocular Indicators of Mental Workload: A Comparison of Scanpath Entropy and Fixations Clustering," Communications in Computer and Information Science, Human Mental Workload: Models and Applications, edited by L. Longo and M. C. Leva, 2019. DOI: 10.1007/978-3-030-32423-0_13.

20. Shannon, C. E., "A mathematical theory of communication," *The Bell System Technical Journal*, Vol. 27, (3), Conference Name: The Bell System Technical Journal, July 1948, pp. 379–423. DOI: 10.1002/j.1538-7305.1948.tb01338.x.

21. Perfect, P., Timson, E., White, M. D., Padfield, G. D., Erdos, R., and Gubbels, A. W., "A rating scale for the subjective assessment of simulation fidelity," *The Aeronautical Journal*, Vol. 118, (1206), August 2014, pp. 953–974. DOI: 10.1017/S0001924000009635.

22. Cooper, G., and Harper, R., "The use of pilot ratings in evaluation of aircraft handling qualities," *NASA Ames Technical Report*, May 1969.

23. Reardon, S., Beard, S., Aponso, B., and Nasa, "Effects of Motion Filter Parameters on Simulation Fidelity Ratings," , May 2014.

24. Roscoe, A. H., and Ellis, G. A., "A Subjective Rating Scale for Assessing Pilot Workload in Flight: A Decade of Practical Use," Technical Report TR 90019, March 1990.

25. "Defence Standard 00-970, Design and Airworthiness Requirements for Service Aircraft, Part 7 – Rotorcraft, Issue 3," , 2010.

26. Štrbac, A., Martini, T., Greiwe, D. H., Hoffmann, F., and Jones, M., "Analysis of rotorcraft wind turbine wake encounters using piloted simulation," *CEAS Aeronautical Journal*, Vol. 12, (2), April 2021, pp. 273–290. DOI: 10.1007/s13272-021-00495-w.

27. Duda, H., Advani, S. K., and Potter, M., "Design of the DLR AVES Research Flight Simulator," AIAA Modeling and Simulation Technologies (MST) Conference, August 2013. DOI: 10.2514/6.2013-4737.

28. Loechert, P., Schmidt, S. O., Jann, T., and Jones, M. G., "Consideration of Tanker's Wake Flow for Helicopter Air-to-Air Refueling," AIAA AVIATION 2021 FORUM, August 2021. DOI: 10.2514/6.2021-2561.

29. Schmidt, S. O., Jones, M., and Löchert, P., "Evaluation of a real-time simulation environment for helicopter air-to-air refuelling investigations," *The Aeronautical Journal*, Vol. 127, (1311), Publisher: Cambridge University Press, May 2023, pp. 754–772. DOI: 10.1017/aer.2022.106.

30. Maibach, M.-J., Jones, M., and Strbac, A., "Development of a Simulation Environment for Maritime Rotorcraft Research Applications," , September 2020.

31. "Airbus A400M conducts major helicopter refuelling certification campaign | Airbus," Section: Defence, October 2021.

32. Gómez, C. G., "Helicopter Aerial Refuelling: A400M Challenges," , 2022.

33. Greiwe, D. H., and Friedrich, M., "Gaze Movements of Helicopter Pilots during real and simulated Take-Off and Landing Maneuvers," Paper presented at Vertical Flight Society International 79th Annual Forum & Technology Display, West Palm Beach, Florida, 16–18 May 2023, 2023. DOI: 10.4050/F-0079-2023-18026.

34. Greiwe, D. H., and Friedrich, M., "A Comparison of Helicopter Pilots' Gaze Movements during Hover Flight in a Real Helicopter and a Full Flight Simulator," Paper presented at 72nd Deutscher Luft- und Raumfahrtkongress, Stuttgart, Germany, 19–21 September 2023, 2023.

35. "Tobii Pro Glasses 3 User Manual v1.19," Vol. 1.

36. Maibach, M.-J., Greiwe, D. H., and Müllhäuser, M., "Helicopter In-Flight Eye Tracking: System Integration Aspects and First Results," Proceedings of the Vertical Flight Society 79th Annual Forum, May 2023. DOI: 10.4050/F-0079-2023-18025.